

Direct Analysis of Trace Phenolics with a Microchip: In-Channel Sample Preconcentration, Separation, and Electrochemical Detection

Muhammad J. A. Shiddiky, Hyun Park, and Yoon-Bo Shim*

Department of Chemistry, Pusan National University, Keumjeong-ku, Busan 609–735, South Korea

A micrototal analytical method assembling in-channel preconcentration, separation, and electrochemical detection steps has been developed for trace phenolic compounds. A micellar electrokinetic chromatography separation technique was coupled with two preconcentration steps of field-amplified sample stacking (FASS) and field-amplified sample injection (FASI). An amperometric detection method with a cellulose–dsDNA-modified, screen-printed carbon electrode was applied to detect preconcentrated and separated species at the end of the channel. The microchip was composed of three parallel channels: first, two are for the sample preconcentration using FASS and FASI methods, and the third one is for the separation and electrochemical detection. The modification of the electrode surface improved the detection performance by enhancing the signal-to-noise characteristic without surface fouling of the electrode. The method was examined for the analysis of eight phenolic compounds. Experimental parameters affecting the analytical performance of the method were assessed and optimized. The preconcentration factor was increased by about 5200-fold as compared with a simple capillary zone electrophoretic analysis using the same channel. Reproducible response was observed during multiple injections of samples with a RSD of <8.0%. The calibration plots were shown to be linear (with the correlation coefficient between 0.9913 and 0.9982) over the range of 0.4–600 nM. The sensitivity was between 0.17 ± 0.001 and 0.48 ± 0.006 nA/nM, with the detection limit of ~100 to ~150 pM based on S/N = 3. The applicability of the method to the direct analysis of trace phenolic compounds in water samples was successfully demonstrated.

A considerable amount of interest in microfluidic devices has recently arisen, because they have the potential advantages of integration, high performance, portability, speed, cost, and minimal solvent/reagent consumption.^{1,2} Despite these advantages, they sometimes suffer from a distinctive limit. The sample is usually present in very low concentration and volume, which makes direct

detection difficult because the low amount of sample may fall near or below the detection threshold for the usual analytical systems.³ One promising alternative to overcome this limitation is on-line sample preconcentration in a microfluidic device.⁴

On-line sample preconcentration in capillary electrophoresis (CE)⁵ can be accomplished with stacking methods based on differences in the electrophoretic mobility of analytes at the boundary of two solutions having different conductivities. Recently, a conventional preconcentration method has been developed by using the field amplified sample injection (FASI) in a low-pH background electrolyte (BGE),⁶ in which the sample was directly injected into the separation column immediately after the injection of a water plug. However, the coupling of the FASI method with a microchannel, which can meet the requirements for the direct analysis of environmental and biological samples with high sensitivity, selectivity, and speed, has not been reported yet.

In-channel sample preconcentration with field amplified sample stacking (FASS) in which a sample solution prepared in a low-conductivity solution is injected into the preconcentration channel filled with a high-conductivity buffer, has been previously developed.^{7–11} When a voltage is applied, the sample experiences high velocity and moves quickly to the boundary between the sample and buffer, consequently forming a concentrated sample zone. However, the implementation of this technique into a microchip suffers from a major difficulty in controlling the sample plug location during the preconcentration step. In solving the difficulty, a complicated channel design,¹² gated injections,¹³ and a porous-polymer film¹⁴ have been previously used. However, these studies were based on optical detection techniques, which are not easy for the miniaturization of the total analytical system. In addition, the enhancement in the sensitivity of these methods

* Corresponding author: Phone: (+82) 51 510 2244. Fax: (+82) 51 514 2430. E-mail: ybshim@pusan.ac.kr.

(1) Harrison, D. J.; Fluri, K.; Seiler, K.; Fan, Z. H.; Effenhauser, C. S.; Manz, A. *Science* **1993**, *261*, 895–897.

(2) Wang, J. *Electroanalysis* **2005**, *17*, 1133–1140.

(3) Yang, H.; Chien, R.-L. *J. Chromatogr., A* **2001**, *924*, 155–163.

(4) Terabe, S. *Anal. Chem.* **2004**, *76*, 241A–246A.

(5) Osbourn, D. M.; Weiss, D. J.; Lunte, C. E. *Electrophoresis* **2000**, *21*, 2768–2779.

(6) Zhu, L.; Tu, C.; Lee, H. K. *Anal. Chem.* **2001**, *73*, 5655–5660.

(7) Lichtenberg, J.; de Rooij, N. F.; Verpoorte, E. *Talanta* **2002**, *56*, 233–266.

(8) de Mello, A. J.; Bread, N. *Lab Chip* **2003**, *3*, 11N–19N.

(9) Jung, B.; Bharadwaj, R.; Santiago, J. G. *Electrophoresis* **2003**, *24*, 3476–3483.

(10) Beard, N. P.; Zhang, C.-X.; de Mello, A. J. *Electrophoresis* **2003**, *24*, 732–739.

(11) Chien, R.-L. *Electrophoresis* **2003**, *24*, 486–497.

(12) Lichtenberg, J.; Verpoorte, E.; de Rooij, N. F. *Electrophoresis* **2001**, *22*, 258–271.

(13) Jacobson, S. C.; Ramsey, J. M. *Electrophoresis* **1995**, *16*, 481–486.

(14) Beckers, J. L.; Bocek, P. *Electrophoresis* **2000**, *21*, 2747–2767.

was between 65- and 1000-fold, which is sometimes not enough for trace analysis in environmental and biological samples. Thus, the demand for a simple, miniature, and sensitive method has arisen. Here, a microchip was fabricated and implemented both FASS and FASI approaches into this chip that can be used to achieve more than 5000-fold increases in sensitivity coupled with electrochemical detection without the use of complex voltage programs.

The most commonly used detection method adapted for on-chip sample preconcentration is UV-visible absorbance detection.^{7,8} However, its sensitivity is limited as a result of the short light path length of the capillary.¹⁵ Although lower detection limits can be obtained with the use of laser-induced fluorescence (LIF) detection, this requires derivatization of the analytes. Electrochemical detection not only shows low detection limits approaching those of LIF detection but also requires relatively simple, compact, low-cost instrumentation. Recently, a micellar electrokinetic separation technique has successfully been coupled with electrochemical detection and used for the analysis of neutral/charged analytes.^{16,17} This coupling also offers relatively high selectivity and fast analysis time.¹⁶ Thus, micellar electrokinetic chromatography with electrochemical detection (MEKC-EC) was used for the separation and detection of preconcentrated trace phenolic compounds.

Since phenolic compounds are toxic, carcinogenic, and immunosuppressive to humans, they are considered environmental pollutants by the U.S. Environmental Protection Agency (EPA).¹⁸ Thus, their trace analysis is of interest in several environmental matrices.¹⁹ Over the past few years, several microchip capillary zone electrophoresis (MCZE)-EC,²⁰ and MEKC-EC^{21,22} methods have been applied to analyze phenolic compounds. The standard analytical methods were not possible for the analysis of trace phenolic compounds without time-consuming preconcentration,²³ even if highly sensitive detection methods were employed. Additionally, conventional electrochemical methods with bare electrodes cannot be applied to detect these compounds because of surface fouling of the electrode by the irreversible adsorption of reaction intermediates and products.^{24,25} Thus, the modification of the electrode surface is also important to attain a stable response and to increase the sensitivity of the electrode. Among many types of electrodes, screen-printed carbon electrodes (SPCEs) have often been used for biosensor applications because of their low-cost, ease of large-scale mass production, flexible design, miniaturiza-

tion, and disposability.^{26–29} Thus, a modified SPCE was employed in this study, in which cellulose–DNA^{30,31} was used as a surface modifier of the SPCE due to its several potential advantages. Cellulose regulated the solubility of DNA molecules in an aqueous media to give the stable electrode surface. The modification of electrodes is also a relatively simple process that entailed screen-printing of the modifier after mixing it with carbon ink. In addition, the cellulose–dsDNA modification of the electrode helps to amplify the sensitivity of the detection because grooves of dsDNA can capture plain structured phenolic compounds through intercalation.

In the present study, a micellar electrokinetic separation method was coupled with two in-channel preconcentration techniques of FASS in basic buffer and FASI in acidic buffer containing micelles of sodium dodecyl sulfate (SDS). A microchannel containing two preconcentration channels to facilitate in-channel preconcentration steps and one separation channel for MEKC separation and detection was fabricated. Amperometry with a cellulose–dsDNA-modified SPCE was applied to detect eight EPA classified phenolic pollutants. Various experimental parameters affecting the analytical performances, such as buffer concentration, pH, water plug length, preconcentration times, detection potential, separation field strength, sample injection times, distance between channel outlet and electrode surface, and SDS concentration, were assessed and optimized. The analytical applicability of the method was investigated for water samples.

EXPERIMENTAL SECTION

Reagents. Carbon, silver, and insulator inks were purchased from Juju Chemical Co. (Japan). Cellulose–dsDNA, SDS, monosodium hydrogen phosphate, disodiumhydrogen phosphate, phosphoric acid, and urea were purchased from Sigma (U.S.A.). 2,4-Dimethylphenol (2,4-DMP), 2,4,6-trichlorophenol (2,4,6-TCP), 2,4,5-trichlorophenol (2,4,5-TCP), 2,3,5-trichlorophenol (2,3,5-TCP), 2,6-dichlorophenol (2,6-DCP), 3-chlorophenol (3-CP), 2-chlorophenol (2-CP), and phenol (P) were purchased from Aldrich (U.S.A.). A standard EPA 8040B mixture of phenols containing nine priority pollutants (2,6-DCP, 2,4,5-TCP, 2-CP, 2,4-DMP, 2,4-dimethylphenol (2,4-DMP), dinoseb (DS), 2,3,4,6-tetrachlorophenol (2,3,4,6-TCP), 3-methylphenol (3-MP), and 4-methylphenol (4-MP)) was obtained from Supelco (U.S.A.) and diluted to desired concentration with distilled water (18.2 k Ω cm⁻¹). The stock solution (100 μ M) of phenolic compounds was prepared in 10% (v/v) methanol, and subsequent dilutions were performed daily in water and filtered with 0.45- μ m Millipore filters (Millipore, MA) (pH was adjusted by adding 2.0 mM NaOH). Phosphate buffer (PBS, 70 mM) (pH 8.5) and 10 mM H₃PO₄ + 10 mM SDS + 1 M urea (low-pH BGE, pH 2.1) were used as stacking buffers in FASS and FASI steps, respectively. Low-pH BGE (10 mM, pH 2.1) and 10 mM PBS (pH

(15) Vilkner, T.; Janasek, D.; Manz, A. *Anal. Chem.* **2004**, *76*, 3373–3386.

(16) Pappas, T. J.; Gayton-Ely, M.; Holland, L. A. *Electrophoresis* **2005**, *26*, 719–734.

(17) Ream, P. J.; Suljak, S. W.; Ewing, A. G.; Han, K.-A. *Anal. Chem.* **2003**, *75*, 3972–3978.

(18) Richardson, S. D.; Ternes, T. A. *Anal. Chem.* **2005**, *77*, 3807–3838.

(19) Chen, G.; Lin, Y.; Wang, J. *Talanta* **2006**, *68*, 497–503.

(20) Wang, J.; Chen, G.; Chatrathi, M. P.; Musameh, M. *Anal. Chem.* **2004**, *76*, 298–302.

(21) Wakida, S.; Fujimoto, K.; Nagai, H.; Miyado, T.; Shibutani, Y.; Takeda, S. *J. Chromatogr. A* **2006**, *1109*, 179–182.

(22) van Bruijnsvoort, M.; Sanghi, S. K.; Hoppe, H.; Kok, W. T. *J. Chromatogr. A* **1997**, *757*, 203–213.

(23) American Public Health Association Standard Methods 5530B–5530D. *Standard Methods for the Examination of Water and Wastewater*, 19th ed.; APHA: Washington, 1995.

(24) Muna, G. W.; Quaiserová-Mocko, V.; Swain, G. M. *Anal. Chem.* **2005**, *77*, 6542–6548.

(25) Gattrell, M.; Kirk, D. W. *J. Electrochem. Soc.* **1993**, *140*, 903–911.

(26) Hart, J. P.; Wring, S. A. *Trend. Anal. Chem.* **1997**, *16*, 889–103.

(27) Darain, F.; Park, S.-U.; Shim, Y.-B. *Biosens. Bioelectron.* **2003**, *18*, 773–780.

(28) Darain, F.; Park, D.-S.; Park, J.-S.; Chang, S.-C.; Shim, Y.-B. *Biosens. Bioelectron.* **2005**, *20*, 1780–1787.

(29) Kim, H.-J.; Cheng, S.-C.; Shim, Y.-B. *Bull. Korean Chem. Soc.* **2003**, *23*, 427–431.

(30) Shiddiky, M. J. A.; Kim, R.-E.; Shim, Y.-B. *Electrophoresis* **2005**, *26*, 3043–3052.

(31) Lee, T. Y.; Kim, H. J.; Moon, J. O.; Shim, Y. B. *Electroanalysis* **2004**, *16*, 821–826.

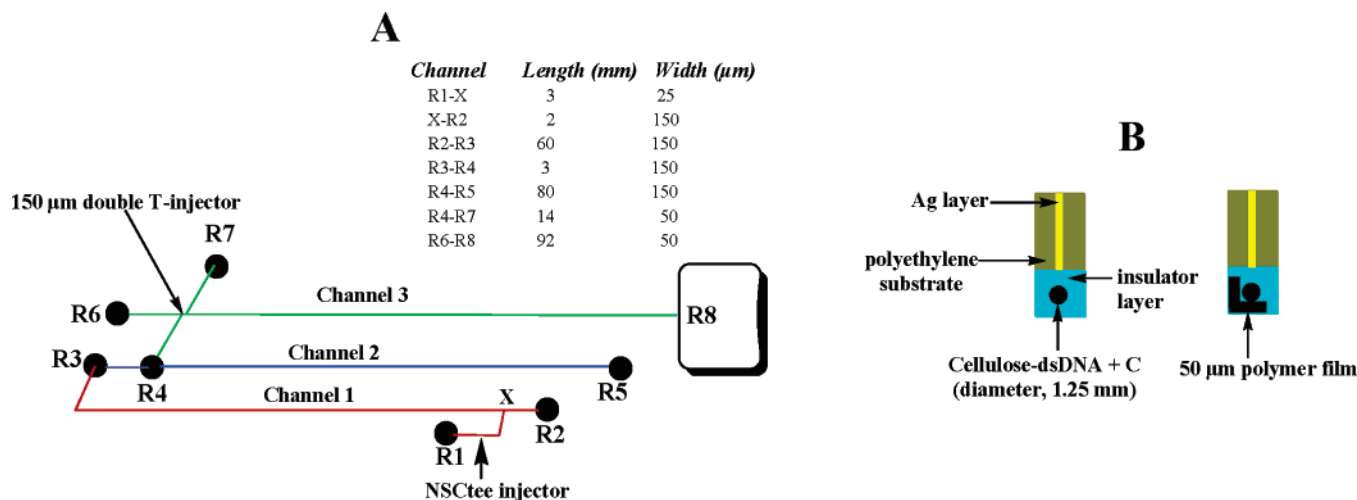


Figure 1. Schematic diagram of the microfluidic device (A) and modified SPCE (B).

7.0) buffers were used in the MEKC-EC step as running and detection buffer, respectively.

Design and Fabrication of the Microchip. The channel pattern of the glass microchip used in this study is shown in Figure 1A. It consists of two parallel preconcentration channels (channels 1 and 2) with a separation channel (channel 3), and each channel is 10 mm from the other. Networks of all channels were designed by using a computer-aided design software package (AutoCad; Autodesk, San Rafael, CA). The separation channel consists of a 150- μm double tee-injector. Channel 1 (from R2 to R3) includes a NSC tee-injector.³² The width of the NSC is 25 μm , which is one-sixth of the channel 1 width. The distances between the injection intersection (X) and the sample waste reservoir 1 (R2) define the sample plug length. This design allows the direct injection of a ~ 2.0 -mm sample plug into channel 1 without any additional leakage control during the FASS step. Channel 2 (from R3 to R5) is 80 mm long and was used for the subsequent FASI step. The insides of all channels are D-shaped and have a depth of ~ 23 μm . Detailed dimensions of all channels are included in Figure 1A. The details of the microfabrication procedure was described previously.³⁰ A homemade Teflon reservoir (i.d. 1.0 mm) was sandwiched onto each hole of the microchip using epoxy glue. The microsyringe needle was connected to the low-pH BGE reservoir (R5) through a fused-silica capillary tube (i.d. 50 μm ; o.d. 150 μm) with epoxy glue. Platinum wires were inserted into the individual reservoirs for contacts of the high voltages.

A Teflon base was fabricated for holding the microchip and for housing the amperometric detector. The detector consisted of a Ag/AgCl reference, a Pt-wire counter, and a SPCE working electrode and was placed in the detection reservoir (R8), where the SPCE aligned at a right angle to the exit of the separation channel outlet. The distance between the channel outlet and the electrode surface was controlled by a screw and a 50- μm polymer spacer,³³ which was confirmed with a microscope (iTPRO, model 3.0, Somatech, South Korea). The design eliminates the permanent attachment of the electrode, which allows fast and reproduc-

ible replacement of the electrode. Additionally, it provides the central positioning of the working electrode, which results in achieving the best sensitivity. The electrochemical experiments were performed with a Kosentech model KST-P1 potentiostat/galvanostat (South Korea). A Spellman CZE 1000R (NY) and a model MHP 50-01B, Imace regulated (South Korea) high-voltage power supply were used for supplying high voltages. All experiments were performed at 25 ± 0.1 $^{\circ}\text{C}$.

Fabrication of the Screen-Printed Electrode. The details of the printing process for the SPCE were described previously.^{30,33} The printing was applied to polyethylene-based films (10 mm \times 30 mm, Figure 1B). Each film consisted of 20 strips; each strip was defined by an individual electrode. First, the Ag conducting layer was printed onto the film, followed by printing of the mixed carbon ink and cellulose-dsDNA working electrode layer (in the case of the bare electrode, only the carbon ink layer was printed onto the film); and finally, an insulating ink layer was printed to cover the junction between the working area and the Ag conducting layer, which gives a definite shape to the working electrode (diameter, 1.25 mm).

Preconcentration and the MEKC-EC Procedure. All experiments were performed using a microchip that had been cleaned with 0.1 M NaOH for 10 min; deionized water for 10 min; and finally, the running buffer for 10 min. After cleaning, channel 1 was filled with 70 mM PBS (pH 8.5) by pumping via R2, where channels 2 and 3 were filled with the low-pH BGE via R5 and the running buffer reservoir (R6), respectively. The schematic diagram of the preconcentration procedure is shown in Figure 2. The sample inlet reservoir (R1) was filled with 100 μL of the sample solution. In the FASS step, sample was injected by applying +100V/cm to the R1 for 20 s. Subsequently, a potential of +200V/cm was applied at R2 for 300 s to start the sample stacking. This operation moves the buffer into channel 1 toward R3, and the analytes accelerate rapidly toward R2 and are stacked at this concentration boundary. During the injection and stacking processes, negatively charged analytes move toward the negative electrode due to the strong electroosmotic flow (EOF) present inside the channel.¹⁰ At the same time, a water plug was injected with a syringe pump (KDS-200, KDS Scientific, U.S.A.) from R5 to the preconcentration reservoir 2 (R4) at a flow rate of ~ 0.1

(32) Zhang, C.-X.; Manz, A. *Anal. Chem.* **2001**, *73*, 2656–2662.

(33) Shiddiky, M. J. A.; Park, D.-S.; Shim, Y.-B. *Electrophoresis* **2005**, *26*, 4656–4663.

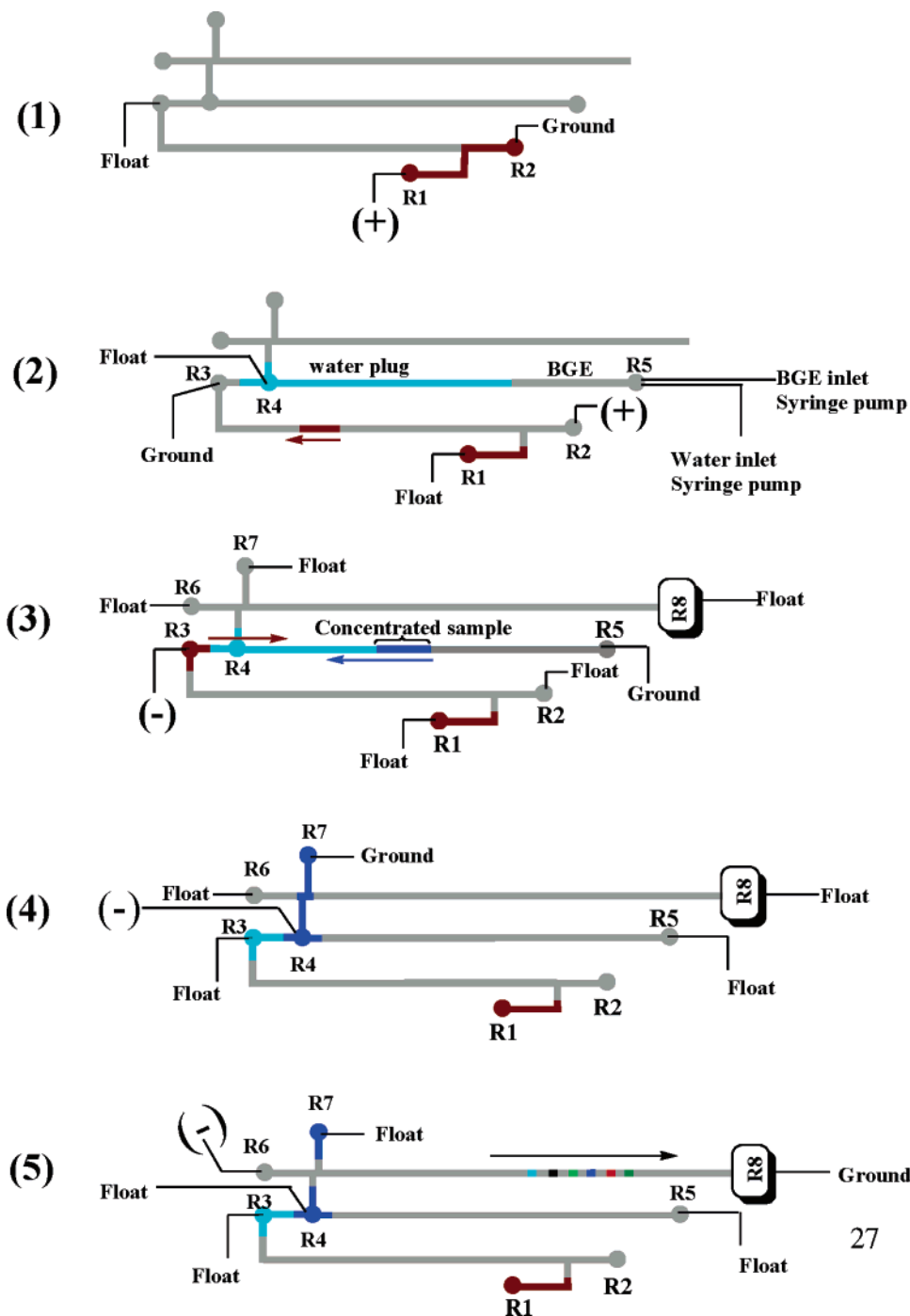


Figure 2. Schematic illustration of the sample preconcentration, separation, and electrochemical detection: (1) Sample loading; a voltage of +100 V/cm was applied to R1 while R2 was grounded and R3 was left floating. (2) FASS step: (i) A voltage of +200 V/cm was applied to R2 while R3 was grounded and R1 and R4 were left floating. (ii) Water/BGE injection: during the FASS step, water was injected hydrodynamically from R5 to R4 in channel 2 at a flow rate of $\sim 0.1 \mu\text{L}/\text{min}$ for 2 min. Immediately afterward, the low-pH BGE was injected for 50 s at the same flow rate. (3) FASI step: Initially preconcentrated sample was then injected into channel 2 by applying a voltage of $-100 \text{ V}/\text{cm}$ to R3 with the R5 grounded, leaving all other reservoirs floating. (4) Sample loading and injection: A voltage of $-200 \text{ V}/\text{cm}$ was applied to R4 with R7 grounded and R3, R5, R6, and R8 floating. Injection was effected by applying an injection voltage of $-200 \text{ V}/\text{cm}$ to R4. (5) Separation and detection: MEKC-EC was performed by applying a separation field strength of $-250 \text{ V}/\text{cm}$ to R6 with R8 grounded and R3, R4, R5, and R7 floating. Amperometric detection potential (DP): $+1.0 \text{ V}$ vs Ag/AgCl.

$\mu\text{L}/\text{min}$ for 2 min to provide a high electric field strength at the injection end. Subsequently, the low-pH BGE was injected for 50 s at the same flow rate and the same position. During this step, an $\sim 60 \text{ mm}$ length of channel 2 was filled with the water plug, and the remaining ($\sim 23 \text{ mm}$) length, with the low-pH BGE. Thereafter, a potential of $-100 \text{ V}/\text{cm}$ was applied to R3 for

$\sim 60 \text{ s}$ to start the FASI step. In this step, the phenolic anions moved rapidly toward R5, passing through the water plug, and stopped when they encountered the low-pH BGE. The low-pH BGE suppresses the EOF³⁴ and acts as a sample trap by trapping

(34) Quirino, J. P.; Terabe, S. *Anal. Chem.* **1998**, *70*, 149–157.

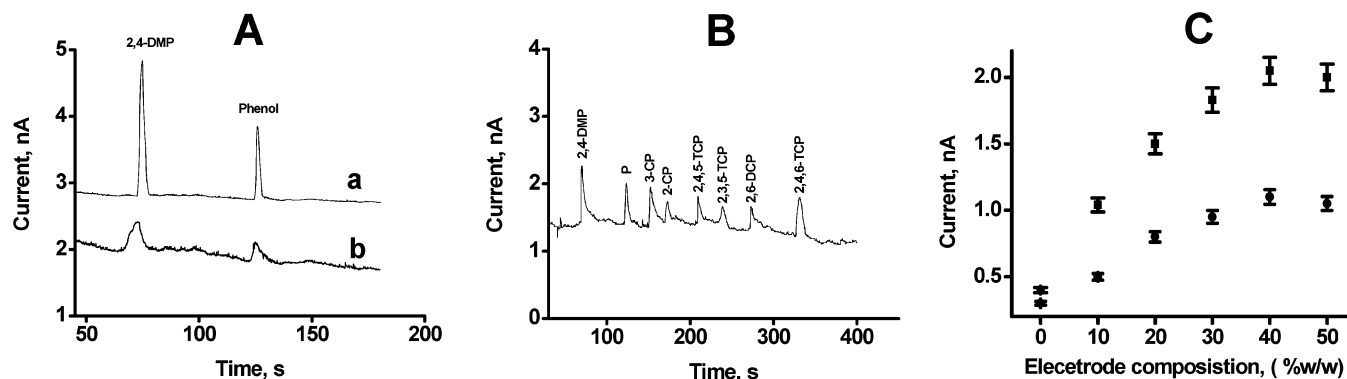


Figure 3. (A) MCZE-EC analysis of 30 μ M 2,4-DMP and P at modified (a) and bare (b) electrodes. (B) MCZE-EC analysis of eight phenolic compounds containing a 15 μ M solution of each compound at a modified electrode. (C) The effect of the electrode composition (cellulose–dsDNA-to-carbon ratio) on the peak current of 30 μ M P (■) and 2-CP (●) at a modified electrode. Separation field strength, +200 V/cm. Sample injection, 3 s at +200 V/cm. DP, +1.0 V vs Ag/AgCl.

the phenolic anions in neutral form.⁶ During this stacking step, the water plug was moving out of channel 2 from R3 because the EOF (toward the R3 reservoir) was controlled by the water plug.³⁵ After ~60 s, the preconcentrated sample zone arrived at R4. Subsequently, MEKC-EC was initiated for the separation and detection of these analytes. In this step, R6 and the sample waste reservoir 2 (R7) were filled with 100 μ L of low-pH BGE, and R8 was filled with 1.0 mL of 10 mM PBS (pH 7.0). The sample was loaded by applying –200 V/cm to R4 for 20 s. Before performing the sample-loading step, 50 μ L of low-pH BGE was added to R4. Thereafter, the channel was pre-electrophoresed for 10 min by applying –200 V/cm to R6. The sample was injected after achieving a stable baseline. Injection was effected by applying –200V/cm to R4 for 3 s. Subsequently, the separation was performed by applying –250 V/cm to R6. For a new run, all new solutions were used following washing steps between runs.

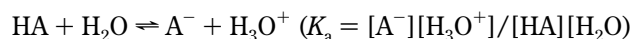
RESULTS AND DISCUSSION

Electrocatalytic Property of the modified Electrode. To illustrate the electrocatalytic activity of the cellulose–dsDNA-modified electrode in comparison to the bare electrode, MCZE-CE was performed and compared. MCZE-CE experiments were carried out using channel 3 of the microchip. A 10 mM phosphate (pH 7.0) buffer was used as detection and running buffers. Figure 3A shows the electropherograms of 30 μ M 2,4-DMP and phenol at bare (b) and modified (a) electrodes. For both electrodes, two peaks were visible at the same migration time. The increased peak current (~5 \times higher) and the decreased half peak width were observed at the modified electrode. The half-peak widths for the 2,4-DMP and phenol at the modified electrode were 2.41 ± 0.25 and 1.62 ± 0.31 s, respectively, which were significantly lower than those obtained at the bare electrode (5.21 ± 0.8 and 3.73 ± 0.5 s, respectively). Using the modified electrode, the separation efficiency for 2,4-DMP and phenol (expressed as the number of the theoretical plates, N) was 830 and 16 909, respectively, whereas 178 and 3189 were calculated from the bare electrode. These values were about 5 \times larger than those obtained at the bare electrode, which might have been attributed to the enhanced electron-transfer process in the oxidation of phenolic moieties through the cellulose–dsDNA layer. There are two possible ways

to increase the sensitivity of the cellulose–dsDNA-modified electrode for the electrooxidation of the phenolic compounds: (i) by increasing their concentration at the electrode interface to aid in capturing the plain structure of phenolic compounds in the grooves of dsDNA through intercalation and (ii) by increasing their electron-transfer rate on DNA molecules.³⁰ Figure 3B illustrates such a characteristic of a cellulose–dsDNA-modified SPCE for the separation and detection of eight phenolic compounds. It showed a slight difference in peak shape, as compared to that of Figure 3A. This can be explained by considering the distance between the electrodes and the channel outlet. Maintaining a constant distance may not be absolute for all electrodes, because this distance can vary a few micrometers electrode to electrode during their replacement and connection steps. This can alter their performance by changing the rate of the (a) post-channel sample diffusion and (b) flow and diffusional spreading across the electrode. However, a relatively flat baseline and a low noise level indicate the more sensitive response of phenolic compounds with the modified electrode.

To determine the optimal content ratio of the cellulose–dsDNA to the carbon ink in the SPCE, the modified electrodes were made using composition ratios of 0, 10, 20, 30, 40, and 50% (w/w). Figure 3C shows the effect of the cellulose–dsDNA content level in the working electrode on the peak current of it. The current for 2-CP and P increased rapidly upon raising the cellulose–dsDNA content from 0 to 30%; after that, the increase was slower and started to level off above 50%. However, the performance of the modified electrode was lower due to the low sensitivity created by the high resistance of the modified electrode when the content of the cellulose–dsDNA was over 40%.^{30,31} Thus, all subsequent experiments employed the 40% cellulose–dsDNA to carbon ratio.

Preconcentration of Phenolic Compounds. Initially, channel 2 was used to preconcentrate the samples by applying FASI at the low-pH BGE. R3 was used as the sample reservoir for these experiments. The dissociation equilibrium between phenolic anions (A^-) and phenol compounds (HA) in water can be written as



When a negative voltage was applied, the phenolic anions in R3

(35) He, Y.; Lee, H. K. *Anal. Chem.* **1999**, *71*, 995–1001.

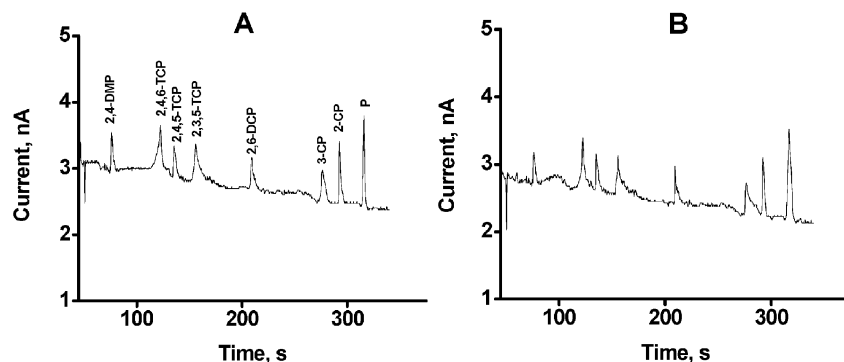


Figure 4. (A) Electropherograms for eight phenolic compounds obtained by the FASI step (A) and by both FASS and FASI steps (B). MEKC-EC conditions: Sample concentration: (A) 15 nM and (B) 2.5 nM each compound. Separation buffer, 10 mM H_3PO_4 + 10 mM SDS + 1 M urea (pH 2.1); detection buffer, 10 mM PBS (pH 7.0); separation field strength, -250 V/cm; injection time, 3 s at -200 V/cm; and DP, $+1.0$ V vs Ag/AgCl.

Table 1. Migration Time, Half-Peak Width, and Separation Efficiency of the Phenolic Compounds at the Modified SPCE Using the Present Method^a

analytes	migration time (t_R , s)	half-peak width ($w_{1/2}$, s)	N^c
2,4-DMP	25.9 ± 0.5	2.1 ± 0.3	~ 800
2,4,6-TCP	71.3 ± 0.6	2.8 ± 0.4	~ 3517
2,4,5-TCP	84.8 ± 0.7	2.4 ± 0.4	~ 6675
2,3,5-TCP	106.3 ± 0.5	2.8 ± 0.4	~ 8160
2,6-DCP	160.8 ± 0.8	2.0 ± 0.3	~ 34415
3-CP	228.8 ± 1.0	4.6 ± 0.7	~ 13729
2-CP	242.6 ± 0.5	2.8 ± 0.3	~ 41680
P	265.5 ± 0.4	3.3 ± 0.4	~ 35860

^a $n = 5$. ^b Peak width at half-maximum point. ^c $N = 5.54 (t_R/w_{1/2})^2$.

moved rapidly toward the boundary of the BGE. The movement of these ions was stopped when they encountered the low-pH BGE, resulting in the formation of neutral phenols by the association reaction of $\text{A}^- + \text{H}^+ \rightarrow \text{HA}$ in the low-pH BGE. The equilibrium in the sample solution was then disrupted. To maintain the equilibrium, the HA dissociated continuously to replenish the A^- ions in the sample solution, consequently associated with HA at the boundary between water and low-pH BGE, thus forming a sharp concentrated sample zone at the boundary. Figure 4A shows a typical electropherogram obtained after the FASI step for a mixture containing a 15 nM solution of each phenolic compound with the modified electrode. Eight peaks were detected with the different migration order as shown in Figure 3B. These differences in the migration times occur at different separation and detection conditions. It is seen that the peak currents in the electropherograms of 3B and 4A are almost the same, when phenols shown in the electropherogram 4A had been diluted to 1000-fold from the solution used to generate the electropherogram 3B. Comparing these two electropherograms, we can conclude that the preconcentration factor was enhanced about 1000-fold by using the FASS step.

To further enhance the concentration extent, we coupled a FASS step with the FASI. In this case, the ~ 2.0 mm sample plug was injected into channel 1 by using the NSC tee-injector. The resulting preconcentrated sample zone arrived at the R3 reservoir within 300 s. Subsequently, FASI was performed. Figure 4B shows

a typical electropherogram obtained after both FASS and FASI steps for a mixture solution containing a 2.5 nM solution of each phenolic compound with the modified electrode. The migration time, half-peak width, and the corresponding separation efficiency are summarized in Table 1. Compared to Figure 4A, the sensitivity increased ~ 4 to 5-fold for each individual compound. This was due to the initial increase in the sample concentration by the FASS step. After both FASS and FASI steps, the concentration enhancement factors were estimated to be in the range of 3890 for 3-CP to 5200 for phenol. This sensitivity enhancement is ~ 4 - to $5\times$ larger than the previously reported highest sensitivity enhancement in a microchip.^{3,9,12}

Optimization of Preconcentration Conditions. The sensitivity enhancement of the FASS step is governed by the stacking efficiency,³⁶

$$E_s = C_1/C_2 = E_1\mu_1/E_2\mu_2$$

where, C_1 and C_2 are the analyte concentration in the original and preconcentrated sample zones, respectively; E_1 and μ_1 are the applied field strength and electrophoretic mobility of the analyte in the sample zone, respectively; and E_2 and μ_2 are the corresponding parameters in the adjacent buffer zone. Thus, the concentration of the buffer affects the stacking efficiency. Figure 5A shows the effect of the PBS concentration in the FASS step on the peak current of 50 nM 2,4-DMP, 2-CP, and P with the modified electrode. In increasing the PBS concentration from 10 to 130 mM (pH 8.5), a gradual increase in the sensitivity was observed. Further increase in the buffer concentration over 70 mM resulted in a decrease in peak currents. This was due to Joule heating, which might have been apparently dominated at the high buffer concentration.¹⁰ Thus, the optimum buffer concentration in the FASS step was considered to be around 70 mM.

The effect of the pH of the sample solution on the current response was examined by increasing the sample pH from 7.0 to 11. Figure 5B shows the effect of pH of the sample solution on the peak current of 50 nM 2-CP and P with the modified electrode. The sensitivity of the electrode increased gradually with increasing pH from 7.0 to 9.0. This was due to the increase in the dissociation of phenolic compounds under basic conditions,⁶ which resulted

(36) Zhang, C.-X.; Thormann, W. *Anal. Chem.* **1998**, *70*, 540–548.

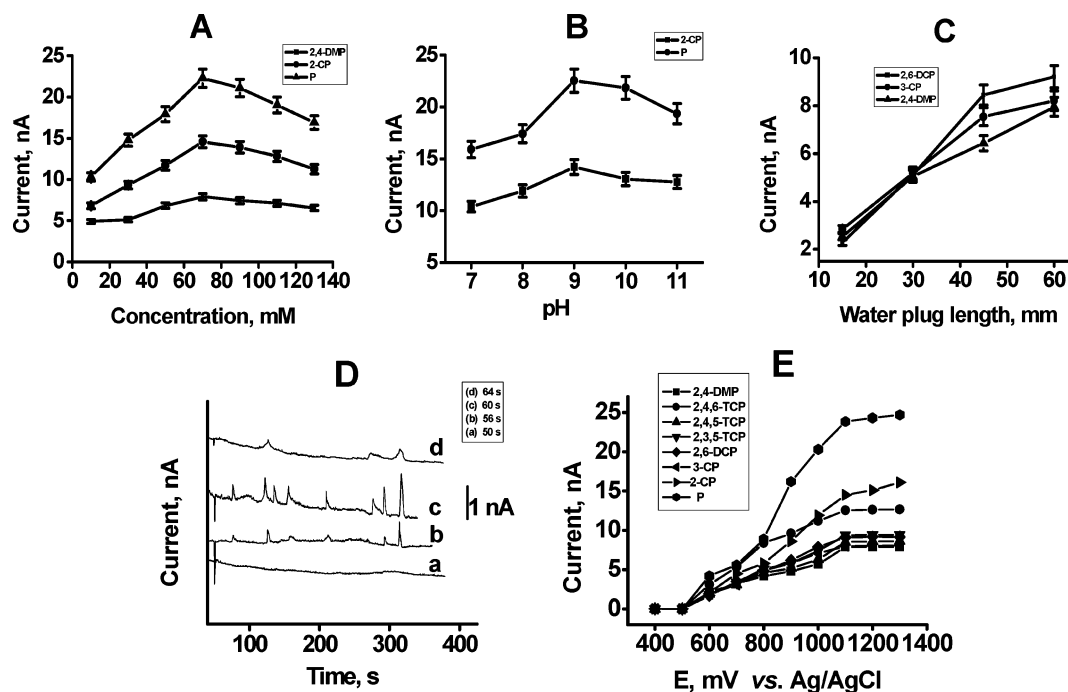


Figure 5. Effects of buffer concentration (A), pH of the sample solution (B), water plug length (C), and preconcentration times (D) on the peak current of the modified electrode and hydrodynamic voltammograms for eight phenolic compounds (E). Sample concentration: 2.5 nM of each compound for D; 50 nM of each compound for A, B, C, and E. Other experimental conditions as in Figure 4.

in the increase in the amount of free phenolic anions in the sample solution and, consequently, increases the stacking efficiency. The application of a pH higher than 9.0 resulted in a decrease in the electrode response, which might be due to the increase in the ionic strength of the sample solution that decreased the conductivity ratio between the sample and adjacent buffer solution (in channel 1) and, thus, decreased the stacking efficiency of the method. Therefore, the optimized pH of the sample solution was 8.5 for all subsequent experiments. Sensitivity of the method was also affected by the sample buffer concentration. When the phenolics were prepared in PBS buffer (pH, 8.5), the concentration enrichment factor decreased gradually with increasing buffer concentration from 1.0 to 10 mM due to the increased conductivity of the sample solution. Thus, the phenolics were prepared in 10% (v/v) methanol.

To increase the concentration enhancement factor of the method, a certain length of water was introduced before starting the FASI step.³⁷ During the electrokinetic injection, the water plug was slowly moving out of the channel from the R3 reservoir, so the plug length should be long enough to hold the phenolic anions. The water plug length, however, should not be too long, which can result in a longer time to arrive at the sample zone at the R4 reservoir. Figure 5C shows the effect of the water plug length in the FASI step on the peak current of 50 nM 2,6-DCP, 3-CP, and 2,4-DMP with a modified electrode. The peak current increased as the water plug increased from ~15 to 60 mm. When the water plug length was ~60 mm, the S/N characteristic of the modified electrode was maximal, with higher separation efficiency. Therefore, a water plug of ~60 mm was used as an optimized water plug length.

The effect of the sample preconcentration time in the FASI step was examined. Figure 5D shows the electropherograms

obtained for preconcentration times of ~50 (a), 56 (b), 60 (c), and 64 s (d). As shown in Figure 5D, all compounds were detected with the modified electrode when time was ~60 s. A stable baseline and maximum separation efficiency was obtained at ~60 s preconcentration time. No peak was detected for ~50 s; however, some peaks were detected in lower response at ~56 and 64 s times, which suggested that a ~50-s preconcentration was not sufficient to bring the sample zone to R4, whereas a 64-s preconcentration time would pump out the sample zone from the R4. Thus, the optimum sample preconcentration time for the FASI step was ~60 s.

Optimization of MEKC-EC Conditions. The effects of the detection potential, separation field strength, injection time, electrode-to-channel distance, and SDS concentration on the peak current of the modified SPCE were studied. Figure 5E displays the hydrodynamic voltammograms for the oxidation of 50 nM 2,4-DMP, 2,4,6-TCP, 2,4,5-TCP, 2,3,5-TCP, 2,6-DCP, 3-CP, 2-CP, and P at the modified electrode. The setup potential of all voltammograms were from +0.6 V, and the peak current gradually increased up to +1.1 V, and leveled off thereafter. The half-wave potential for all analytes was between +0.8 and +1.0 V. An increase in the baseline current, its slope, and the corresponding noise were observed at a detection potential higher than +1.0 V. The high background current leads to an unstable baseline, which is disadvantageous in achieving a highly sensitive and stable detection. Thus, a detection potential of +1.0 V was employed for all subsequent experiments.

The separation field strength affects the migration time, peak current, and the separation efficiency of analytes. The migration time decreased upon increasing the field strength. A larger initial drift of the baseline was observed for the higher field strength, indicating an incomplete isolation at the high separation field strength. The separation efficiency increased upon negatively

(37) Chien, R. L.; Burgi, D. S. *J. Chromatogr.* **1991**, *559*, 141–152.

Table 2. Analytical Performance of the Method

analytes	C ^a	response precision (% RSD, <i>n</i> = 5)	dynamic range (nM)	detection limit ^b (pM)
2,4-DMP	4500	6.3	0.5–410	~120
2,4,6-TCP	5100	5.8	0.5–300	~100
2,4,5-TCP	4700	6.2	0.75–300	~150
2,3,5-TCP	4230	5.7	0.5–300	~100
2,6-DCP	4400	7.6	0.75–300	~120
3-CP	3890	6.7	0.75–380	~150
2-CP	4950	5.9	0.75–500	~150
P	5200	5.2	0.4–600	~100

^a C = Concentration enhancement factor. ^b Estimated detection limits, based on S/N = 3.

increasing the field strength from –100 to –250 V/cm. Further increases in the field strength over –250 V/cm resulted in a decrease in separation efficiency.^{38,39} A maximum S/N characteristic with the higher separation efficiency was observed at –250 V/cm. Thus, a separation field strength of –250 V/cm was chosen for all subsequent separations.

The sample injection time for the MEKC-EC step affects both the peak current and peak shape at the modified electrode. The peak current and the half-peak width increased as the injection time increased from 1 to 6 s. When the injection time was 3 s, the half-peak width was the minimum with the maximum peak current. Further increase in the injection time resulted in an increase in half-peak width and, thus, a decreased separation efficiency. Therefore, 3-s was selected as the optimized injection time. The influence of the electrode-to-channel distance in the MEKC-EC step was examined. When the electrode-to-channel distance increased from 50 to 200 μm , a gradual decrease in the current response with an increased half-peak width was observed.^{33,39} Thus, a working electrode was placed at a distance of 50 μm from the channel exit.

To optimize the MEKC-EC performances with the modified electrode, the effect of the SDS concentration in the running buffer (the critical micellar concentration is $\sim 8.1 \text{ mM}$ ⁴) was studied in the range of 2.5–20 mM. The migration times of all the compounds increased with increasing concentration of SDS attributed to increased analyte–micelle interaction. This suggests an increased capacity of the micelles for analyte solubilization as the concentration increased. However, a concentration of SDS lower than 7.5 mM was not suitable for separating all of the compounds. It was likely that these compounds might adsorb to the channel wall at the low SDS concentration. At the 10 mM SDS concentration, all of the compounds were separated in better resolution. Thus, MEKC-EC experiments employed a low-pH BGE containing 10 mM SDS (pH 2.1).

Analytical Performance. Under the optimized conditions, the concentration enhancement factor, linear dynamic ranges, detection limits, and the reproducibility of the method were calculated and are summarized in Table 2. The reproducibility of the analysis clearly indicates a negligible surface fouling of the modified electrode. However, a slight variation of the migration times (RSD

< 4.0%, *n* = 5) was observed, which was due to (a) the changes in the concentration of the running buffer in the separation channel and (b) the contamination of the electrode surface caused by the repetitive sample injections. The detector-to-detector reproducibility was <3.5%, even when the same preparation conditions were used, which might have been attributed to the difficulty of controlling homogeneity of the modified surface and the exact amounts of cellulose–dsDNA modifier to the carbon powder during the electrode preparation steps. The stability of the electrode was examined using 15 repetitive injections of 50 nM solutions of the phenols. The consecutive injections displayed a steady decrease in the peak response (with a 45% decrease in the initial peak areas; RSD, 12%; *n* = 15), which were most likely due to the polymeric film formation on the electrode surface.^{24,25}

The calibration plots (not shown) for all analytes were found to be linear (with the correlation coefficient between 0.9913 and 0.9982) over the range of 0.4–600 nM. The sensitivity of the modified electrode for 2,4-DMP, 2,4,6-TCP, 2,4,5-TCP, 2,3,5-TCP, 2,6-DCP, 3-CP, 2-CP, and P were 0.18 ± 0.014 , 0.25 ± 0.003 , 0.17 ± 0.001 , 0.21 ± 0.002 , 0.19 ± 0.002 , 0.17 ± 0.001 , 0.35 ± 0.004 , and $0.48 \pm 0.006 \text{ nA/nM}$, respectively, with detection limits of ~120, 100, 150, 100, 120, 150, 150, and 100 pM, respectively, on the basis of S/N = 3 (95% confidence level, *k* = 3, *n* = 6). These results are much lower than those obtained by the other groups using the liquid-phase microextraction,⁶ flow-injection,⁴⁰ and FASI⁴¹ analysis methods and comparable to those obtained by solid-phase extraction²⁴ and HPLC⁴² analysis methods. The low detection limit, wide linear dynamic range, and good reproducibility of the method enabled it to be successfully employed for the analysis of trace phenolic compounds in environmental samples.

Application to Standard and Real Samples Analysis.

Because our final goal is to develop a fast, sensitive, and simple method for the analysis of environmental and biological trace target analysis, it is important that this method can be used to analyze relevant samples. Before performing the real sample analysis, a 10 ng/mL of EPA 8040B phenols mixture was analyzed using the method. All peaks were separated and detected at the migration times of ~26.1, 38.4, 55.7, 84.9, 118.5, 142.2, 160.5, 181.8, and 243.1 s for 2,4-DMP, 3-MP, 4-MP, 2,4,5-TCP, 2,3,4,6-TCP, DS, 2,6-DCP, 2,4-DNP, and 2-CP, respectively. The real samples were collected from tap water (water service pipes, Busan City) and surface water (upper stream of a local canal), and their phenolics concentrations were determined with this method within the same day. Before performing experiments using the present method, untreated samples were filtered, and their pHs were adjusted to 8.5 by adding 2.0 mM NaOH. Figure 6A, B shows the electropherograms for the tap and surface water samples, respectively. In the surface water samples, all peaks were separated from one another and were detected with the same migration times as shown in Figure 4B. In the tap water samples, some of the target peaks were separated and detected with approximately the same electrophoretic performances as shown in Figure 6B. The peaks in Figure 6A, B were confirmed by spiking the real samples with individual standard phenols (10 nM). The average recovery (*n* =

(38) Pumea, M.; Wang, J.; Grushka, E.; Polsky, R. *Anal. Chem.* **2001**, *73*, 5625–5628.

(39) Shiddiky, M. J. A.; Rahman, M. A.; Park, J.-S.; Shim, Y.-B. *Electrophoresis* **2006**, *27*, 2951–2959.

(40) Kuban, P.; Berg, M.; García, C.; Karlberg, B. *J. Chromatogr., A* **2001**, *921*, 163–170.

(41) Marti, D.; Borrull, F.; Calull, M. *J. Chromatogr., A* **1997**, *788*, 185–193.

(42) Terashima, C.; Rao, T. N.; Sarada, B. V.; Tryk, D. A.; Fujishima, A. *Anal. Chem.* **2002**, *74*, 895–902.

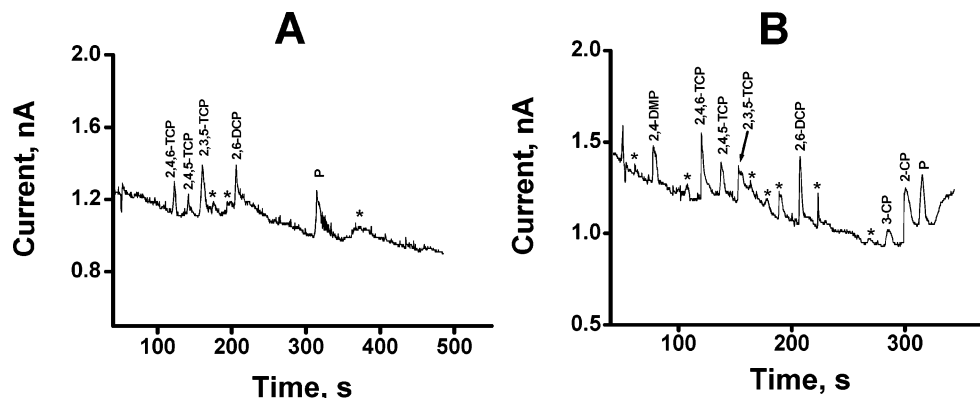


Figure 6. Electropherograms of the tap (A) and surface (B) water samples. Experimental conditions as in Figure 5.

4) for all compounds was from ~ 94 to 105%. However, apart from these target peaks, there are some additional peaks in both electropherograms, possibly due to the other trace phenolic compounds or other slightly acidic compounds present in water samples being preconcentrated during the processes and detected at +1.0 V with the modified electrode. A relatively unstable baseline, which is often observed for the analysis of surface water by applying a preconcentration method, resulted from the modified electrode. To examine the interference of the ionic species present in the real samples on the sensitivity of the method, we spiked surface and tap water samples with 10 ng/mL of the EPA 8040B phenols mixture. All phenolics in the 8040B mixture and real samples were successfully detected and separated (not shown) with good reproducibility ($n = 3$) in migration times ($< 3.2\%$) and peaks currents ($< 8.0\%$). The recoveries for 2,6-DCP, 2,4,5-TCP, 2-CP, and 2,4-DMP were also the same as those obtained from addition of individual standard phenols. The estimated concentrations of the phenolics in tap and surface water samples were in the range of ~ 0.70 nM for 2,4,5-TCP to ~ 1.1 nM for 2,3,5-TCP and ~ 0.50 nM for 3-CP to ~ 1.5 nM for 2,6-DCP, respectively. These levels are much lower than those of the U.S. EPA's recommended maximum allowable levels for phenolic compounds in publicly supplied water.⁴³ Thus, the present method can be used for rapid analysis of water samples from sites that are suspected to be contaminated by the phenolic compounds.

CONCLUSIONS

We have developed a simple, sensitive, and fast method for the preconcentration, separation, and electrochemical detection

of phenolic compounds. This method uses two preconcentration channels to facilitate in-channel sample preconcentration by FASS and FASI steps and one separation channel for MEKC separation and electrochemical detection with the cellulose-dsDNA modified electrode. The preconcentration factor was increased by ~ 5200 -fold, as compared to the MCZE-CE analysis, with the modified electrode. The optimum detection potential for all analytes was about +1.0 V. The sensitivity of the modified electrode was in the range of 0.17 ± 0.001 to 0.48 ± 0.006 nA/nM with a detection limit of ~ 100 to ~ 150 pM ($S/N = 3$). The modified electrode displays an improved sensitivity, stability, and resolution, as compared to a bare electrode, reflecting the electrocatalytic activity and resistance to surface fouling of the modified electrode. The use of such an electrode has great promise in being mass-produced as a single-use analytical system for environmental pollutants. The low detection limit, high sensitivity, simplicity, and reproducibility of the method allows for the analysis of phenolic compounds in water samples. It can also be used for analyzing other electrochemically active and slightly acidic compounds. Work is currently in progress in these directions.

ACKNOWLEDGMENT

This work was supported by the Ministry of Environment as The Eco-Technopia 21 Project and the Ministry of Health and Welfare of Korea (Grant 02-PJ3-PG6-EV05-0001).

Received for review March 31, 2006. Accepted August 1, 2006.

AC0606002

(43) <http://www.epa.gov/ebtpages/watewaterhealthadvisories.html>.